

# PILOT PRODUCTION OF FAÇADE PANELS: VARIABILITY OF MIX DESIGN

MAJDA PAVLIN, BARBARA HORVAT, VILMA DUCMAN

Slovenian National Building and Civil Engineering Institute, Ljubljana, Slovenia  
majda.pavlin@zag.si, barbara.horvat@zag.si, vilma.ducman@zag.si

**Abstract** As part of the WOOL2LOOP project, the Slovenian National Building and Civil Engineering Institute (ZAG), in collaboration with Termit d.d. were responsible for the production of façade panels. An initial mix design was developed at ZAG, where alkali-activated façade panels were produced, primarily from stone wool waste, while production took place at Termit. The mix design was changed twice during the pilot production, before a final product with suitable durability was developed. A compressive strength of up to 60 MPa and bending strength of approximately 20 MPa was achieved. The mechanical properties, however, varied, due to the unevenly milled batches of the milled mineral wool. Milling on a larger scale is very challenging, and it is difficult to obtain consistent quality of the milled material. Once the correct curing process had been found, however, the panels produced showed good performance. Moreover, the results from leaching tests showed that the elevated concentrations of certain elements (Cr, As and Mo) did not exceed the legal limits for non-hazardous waste.

**Keywords:**  
waste mineral  
wool,  
façade panels,  
alkali-activated  
material,  
recycling,  
leaching,  
mechanical  
properties

## 1 Introduction

Mineral wool is one of the most widely used insulation materials in the world. As a result, its disposal poses a major problem at the end of its use, taking up a lot of space in landfills due to its low density. In 2020, the European Union generated approximately 2.55 million tons of mineral wool waste, which represents only about 0.2% of the total amount of construction and demolition waste produced in the European Union. Most construction and demolition waste is recyclable, while mineral wool is considered to be non-recyclable (Väntsi and Kärki, 2014). There is therefore an urgent need to find a way to recycle, reuse or recover these wastes. Mineral wool is usually divided into two categories - stone and glass wool - which differ in terms of both their chemical composition and the raw materials used in their production (Müller et al., 2009; Kowatsch, 2010). Stone wool accounts for about 70% of the mineral wool produced worldwide (Väntsi and Kärki, 2014). Under the Wool2Loop project the consortium has developed and produced various products with alkali activation technology, using mineral wool as the main raw material (precursor). Alkali activation is based on a chemical reaction that can produce end products that have similar or better properties than concrete or ceramic-type products. Some studies have already been conducted where mineral wool was alkali-activated, either alone or in combination with other co-binders (Yliniemi et al., 2016; Kinnunen et al., 2017). Although, theoretically, mineral wool waste is an ideal starting material, because almost 100% of this waste is in the amorphous phase, in reality not all fibres dissolve during alkali activation (Pavlin et al., 2021a). This should be taken into account, because problems with efflorescence can occur if too much of the alkali activator is added.

In the present work, architectural façade panels were developed. The selected mix design (Pavlin et al., 2022) consisted of mineral wool waste as the main raw material, with local slag (a mixture of electric arc furnace slag and ladle slag), metakaolin and lime added as co-binders. Mix design developed and selected in the lab was modified two times. The prepared façade panels was monitored by measuring the mechanical properties of the alkali-activated material (AAM), the particle size distribution in randomly selected samples, mineralogy, open porosity, the degree of alkali activation and leaching parameters used to evaluate the environmental impact.

## 2 Material and methods

**Sample preparation:** Stone wool (SW) was used as the primary precursor for the preparation of façade panels. Milled material was obtained from the company ISOMAT (Slovenia). A sodium silicate obtained from Termit d.d. (sodium silicate activators with a molar ratio-module of approximately  $\text{SiO}_2/\text{Na}_2\text{O} = 2.5$ ; and mass percent 11.9%  $\text{Na}_2\text{O}$ , 28.5%  $\text{SiO}_2$ ) was used for the alkali activation. Various co-binders, including local slag (S; commercially available electric arc furnace slag mixed with ladle slag and branded as secondary by-product EKOMINIT; milled and sieved below 125  $\mu\text{m}$ ), metakaolin (MK; used as received) and lime (L; used as received) were also added to the mineral wool precursor. As aggregate (AG) quartz sand (MP-MIX) from Termit d.d. was used for all prepared mix designs. After mixing all the dry precursors together, sodium silicate was added and mixed until the slurry was completely wet, and then the slurry was poured into moulds made of silicone or urethane rubber. For optimisation of mix design, at first, the samples were cured at room temperature in closed PVC bags to hinder dehydration. Then after three days, the façade panels were exposed to an elevated temperature (60 °C at 30, 60 or 90% humidity; humidity chamber POL-EKO APARATURA, Poland).

**Analysis of the precursors and AAMs:** Chemical (X-ray fluorescence, XRF; Thermo Scientific ARL Perform'X Sequential XRF) and mineralogical (X-ray powder diffraction, XRD; Empyrean PANalytical X-ray Diffractometer, Cu X-Ray source) analyses of SW, S, M and L were conducted. All the precursors were dried, milled and sieved to below 125  $\mu\text{m}$  prior analyses. XRF measurements were performed on molten discs and analysed using UniQuant 5 software. The data measured are provided in Table 1.

**Table 1: Chemical composition of the precursors (stone wool, lime, metakaolin and local slag) used for the alkali activated façade panels.**

Chemical composition of precursors	$\text{SiO}_2$ (wt%)	$\text{Al}_2\text{O}_3$ (wt%)	$\text{Na}_2\text{O}$ (wt%)	$\text{CaO}$ (wt%)	$\text{MgO}$ (wt%)	$\text{Fe}_2\text{O}_3$ (wt%)	LOI (950 °C)
Stone wool (SW)	38.4	17.2	2.00	16.1	11.6	6.45	4.60
Lime (L)	1.86	2.05	0.30	68.2	2.07	0.10	24.8
Metakaolin (M)	68.1	25.2	0.09	0.45	0.16	2.21	2.25
Local slag (S)	13.7	5.20	0.28	27.9	23.3	4.64	20.5

The XRD patterns were solved using X'Pert Highscore plus 4.1 software. Rietveld refinement was performed with an external standard (corundum,  $\text{Al}_2\text{O}_3$ ) to estimate the content of amorphous content and minerals. XRD spectra of the precursors used in the alkali activation process are provided in **Figure 1**.

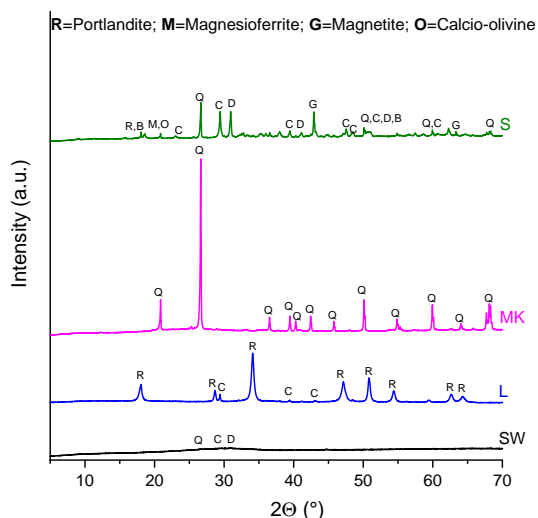


**Figure 1: Diffractograms of the precursors (SW, L, MK and S) used for preparation of the façade panels.**

Source: own.

Open porosity of alkali-activated façade panels was determined using mercury intrusion porosimetry (MIP). Small representative fragments about  $1\text{ cm}^3$  in size were dried for 24 h before measurement and then analysed using Micromeritics® Autopore IV 9500 equipment (Micromeritics, Norcross, GA, USA).

28 days after placing samples in the moulds the mechanical strength (bending and compressive) of the AAMs was measured using a compressive and bending strength testing machine (ToniTechnik ToniNORM).

The presence of toxic elements in leachates was evaluated after 28 days according to the European standard SIST EN 12457-2. The AAM was crushed to a grain size of below 4 mm and added to a glass bottle containing deionised water using a solid:liquid mass ratio of 1:10. The suspensions were rotated around the vertical axis for 24 h at room temperature conditions, and then filtered to below  $0.45\ \mu\text{m}$ . An

aliquot of the coloured liquid fraction obtained (Figure 2, the typical yellow-brown colour is a consequence of organic resin or other organic compounds present on the surface of the milled waste mineral wool) was digested in the microwave, then the clear solutions prepared were used to determine the amount of metals released using an inductively coupled plasma mass spectrometer (ICP-MS, Agilent 7900). The results were compared to the total amount of toxic trace and minor elements measured in the precursor, as well as to figures from the legislation (Decree on Waste Landfill (Official Gazette of Republic Slovenia, 2014)).

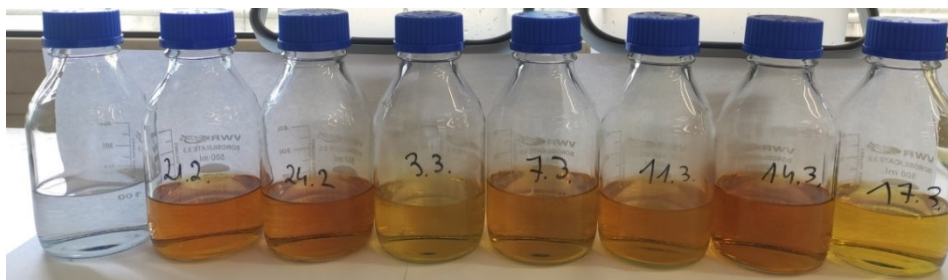


**Figure 2:** Leachates from the alkali activated façade panels obtained following filtration to below 0.45  $\mu\text{m}$ . The transparent liquid in the bottle on the left is a blank, without the addition of a sample.

Source: own.

### 3 Results

#### 3.1 The results of milling process

The mineral wool was pre-milled by a Slovenian company, and the mass ratio of the finest particle size ( $< 63 \mu\text{m}$ ) over the time of the study is shown in Figure 3. When the development of initial mix design (described in details in 3.2.) had started (i.e. mix design 1), the finest fraction of mineral wool waste accounted for more than 60 wt% of total content (Figure 3; milled mineral wool samples 1-4). When upscaling mix design 1, the slurry was too liquid, and the amount of sodium silicate and waste mineral wool was adjusted, and this led to development of mix design 2. After changing the grinding parameters in the company that performed this, the quality of the milled mineral wool decreased (Figure 3; milled mineral wool sample 5) and production of the façade panels was faced with various problems, starting with poor

workability of mix design 2. Besides problems with initial fresh mixture, the already cured panels exhibited curvature, high structural porosity and the occurrence of the efflorescence. The situation became even worse with the milled mineral wool samples 6-8 (Figure 3), where the proportion of the finest fraction represented only a few mass percent of the total content. From that point forward, additional milling was implemented by Termit using a concrete mixer (i.e. ball milling). With double-milled mineral wool it was possible to prepare mix design 1 again, but to minimize the efflorescence, mix design 3 was developed. This mixture was then used in the pilot production.

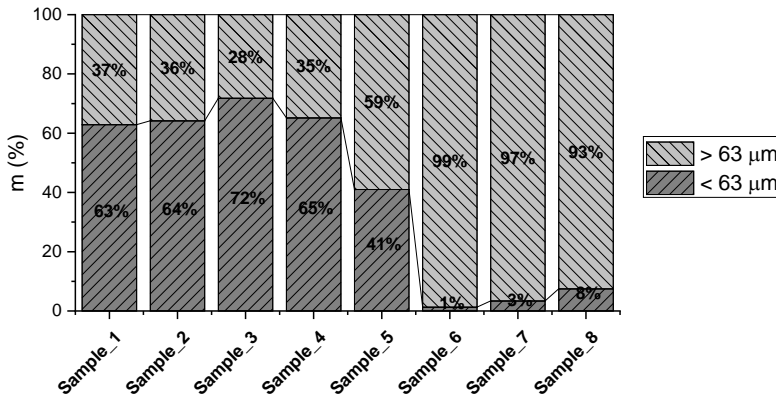


Figure 3: The particle size distribution of the finest fraction (< 63  $\mu\text{m}$ ) versus other fractions (> 63  $\mu\text{m}$ ) in the (pre)milled mineral wool.

Source: own.

### 3.2 Preparation of façade panels: optimisation of selected mix design

The façade panels prepared from mineral wool and other co-binders need to have suitable mechanical properties, and be both durable and environmentally-friendly (in terms of their parameters regarding leaching toxic metals and other toxic substances). Following use of the initial mix design (mix design 1) in the pilot production, some modifications were then made to the mix design at the beginning of pilot production (mix design 2; the mixture was too liquid so less sodium silicate was used and the proportion of mineral wool was increased, as shown in Table 2). After that, based on many problems with the façade panels with respect to curvature,

porosity, efflorescence, workability and demoulding time, the mix design had to be modified again during the pilot production. The last change in the mix design (to developed mix design 3) was made mainly due to the observed curvature and difficult mixing of the very viscose slurry while aiming for perfect wetting of the pulverized precursor's particles (poor workability of the mixes as a result of the unevenly ground mineral wool batches, Figure 3). The original mix design developed in the lab and used for pilot production (mix design 1), the modified mix design (mix design 2), and the final mix design (mix design 3), are defined in Table 2. Mix designs 1 and 2 were cured at room temperature, while mix design 3 was cured for three days at room temperature covered with PVC to hinder the dehydration and allow slow-reacting precursor enough time for initial curing before demoulding (Pavlin et al., 2021a), and then at 60 °C and 60% humidity on level metal mesh for uniform drying of all 6 panel's sides. There are some differences between the various mixes; due to the presence of efflorescence, for example, NaOH was removed from the mix design 3 and the amount of sodium silicate reduced (in mix design 2 and 3), also the amount of used waste mineral wool differ (Table 2).

The compressive and bending strengths of the initial mix developed in the laboratory (mix design 1) cured at room temperature for 28 days were  $(42.5 \pm 2.7)$  MPa and  $(14.3 \pm 2.1)$  MPa, respectively, while the compressive and bending strengths of mix design 2 (also cured at room temperature) were lower  $(33.3 \pm 3.1)$  MPa and  $(11.3 \pm 0.5)$  MPa, respectively. Mix design 3, cured three days at room temperature and three days at 60 °C and 60% humidity, showed similar mechanical properties to mix design 1 after 28 days of curing at room temperature, with a compressive strength of  $(41.0 \pm 7.1)$  MPa and a bending strength of  $(15.3 \pm 0.4)$  MPa.

The workability of mixtures is very important, especially at the industrial level of pilot production. It was evaluated using a slump test by measuring the spread of the mortar. The data for prepared mixtures can be found in Table 2 (slump test; the good workability of prepared mortars is usually in the range of 165-185 mm (Pavlin et al., 2022)). Workability depends on the particle size of the starting materials as a result of the grinding process. In the case of mineral wool, a higher amount of the fraction  $> 63 \mu\text{m}$  - larger particles, require more liquid (sodium silicate) to achieve the desired workability of the mixture, and therefore mixing was difficult with the same amount of sodium silicate and larger particles, and vice versa, smaller particles

require less liquid. Moreover, the dense mixture did not result in any changes in the spreading of the slurry in the slump test (the diameter measured on the spreading table remained the same). Mix design 1 contained the highest amount of sodium silicate and showed the highest spread whereas mix design 2 and 3 had the same spread (the results of slump test in Table 2).

**Table 2: The original mix design (mix design 1), developed in the lab of ZAG, the modified mix design (mix design 2) and mix design currently in use (mix design 3).**

Mix design	SW (g)	Sodium silicate (g)	NaOH (g)	L (g)	M (g)	S (g)	AG (g)	Slump test (mm/mm)
1 (original)	29.9	42.7	0.47	0.85	7.67	4.26	14.2	172/183
2	33.9	39.8	0.46	0.97	7.47	3.59	13.8	165/170
3 (current mix)	33.1	37.6	/	0.95	8.51	4.72	15.1	165/170

At the beginning of the pilot production, panels were demoulded after one day (mix design 1) (Pavlin et al., 2022). Using batches of milled mineral wool with a higher mass percentage of big particles ( $> 63 \mu\text{m}$ , Figure 3) this was no longer possible due to the change in the particle size after milling. Therefore, the curing conditions were optimized; first, curing was performed at room temperature, then different conditions were tested (60 °C and humidity of 30, 60 or 90% (Pavlin et al., 2021b)). We also performed experiments at 40 °C, but the mechanical properties were lower and the curing times should be longer, therefore those results were excluded (Pavlin et al., 2021b). The results of the mechanical properties after testing different humidity at 60 °C can be found in Figure 4.

Panels cured at 60 °C and 30% humidity were not suitable and showed little curvature. A humidity of 90% was too aggressive for the curing oven, which was evident from the damaged support mesh caused by the high alkaline vapour resulting from the alkali activation process. 60 °C and 60 % humidity were selected as the most suitable curing conditions at which the façade panels did not exhibit the curvature. At the same time, tests were carried out with different amounts of lime, with the mixtures containing 1, 2, or 3 wt% lime. However, with 1 wt% lime, the specimens could not be demoulded after three days of curing at room temperature and exhibited curvatures, while with 3 wt% lime, mixing the mixtures was difficult due to the too fast hardening. Mix designs 1 and 2 with 2 wt% of lime showed no



curvature, but mix design 2 was difficult to prepare due to the viscous slurry. Therefore, mix design 1 with 2 wt% of lime was taken for further optimisation.

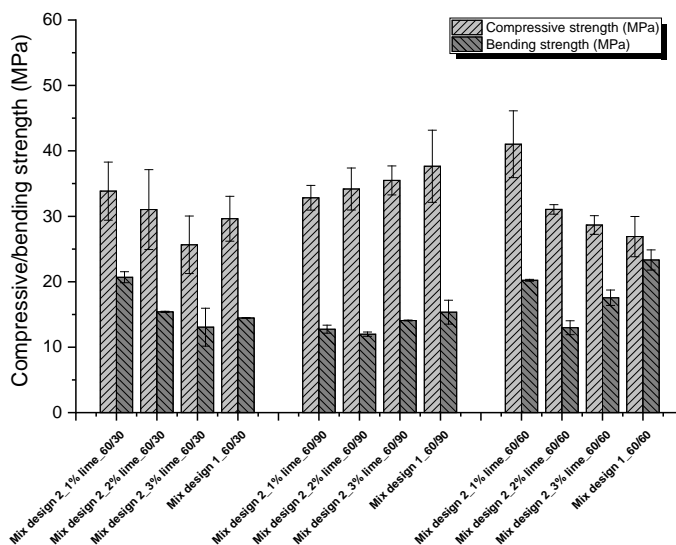


**Figure 4:** Samples cured three days at room temperature in closed bags and then three days at 60 °C with different humidity (30, 60 or 90%). 1, 2 or 3 wt% of lime were added in the mix design 2. Sample mix design 1 had 2 wt% of added lime.

Source: own.

After selecting the curing conditions (60 °C and 60% humidity), tests regarding the time of the additional milling and the variations in the amount of sodium silicate and NaOH were performed, which are shown in Figure 5. Mineral wool from sample batches 6-8 was used for this experiment (Figure 3). The workability of the mixtures, evaluated by the slump test, is presented in Table 3. Initially, mix design 1 was selected and mineral wool sieved below 125 µm was used. The workability of this mixture was suitable for further use, but unfortunately, the panel showed curvature. Then tests were carried out with different milling times (2, 4, 6 and 8 hours of additional grinding in the concrete mixer). The use of the wool after 2 and 4 hours of additional grinding was not suitable (the mixture was too dense). After 6 hours, the workability was better, but the mixture was still too viscous to be useful in the pilot production. On the other hand, after 8 hours of grinding, the mixture was too liquid, therefore the amount of sodium silicate was reduced. The sample "Mix design

1\_milled 8h\_lessSS2x" showed good workability and no curvature. However, to decrease the efflorescence, NaOH was removed from the mix design and therefore "Mix design 1\_milled 8h\_lessSS2x\_no NaOH" was selected as a mixture for further production of panels labelled as "mix design 3". "Mix design 2\_no NaOH" showed good workability, but was not selected, because its slurry showed adhesiveness to the flow table (used for the slump tests) and was therefore not useful for industrial production (mixture design 2 was added for comparison purposes only; the results of slump tests in Tables 2 and 3 differ due to the additional grinding process shown in Table 3 in the case of mix design 2).

**Table 3: Spread of the prepared panels.**

Sample	Slump test (mm/mm)
Mix design 1 sieved<125 um	168/165
Mix design 1 milled 2h	Too viscose
Mix design 1 milled 4h	125/128
Mix design 1 milled 6h	162/168
Mix design 1 milled 8h	Too liquid
Mix design 1 milled 8h_lessSS	201/203
Mix design 1 milled 8h_lessSS2x	173/175
Mix design 1 milled 8h_lessSS2x_no	<b>165/170</b>
Mix design 2	182/192
Mix design 2 no NaOH	173/178

However, the mechanical properties of the prepared samples (Figure 5) did not differ that much, considering that some of the mixtures were too viscose and some too fluid.

The lowest compressive strength (about 30 MPa) was exhibited by the sample with mineral wool additionally ground for 2 hours (due to the poorer dissolution of amorphous Si and Al owing to the lack of liquid - sodium silicate). As mentioned earlier in the text, bigger particles needed more liquid and therefore mixing is difficult. Mix design 2 exhibited the lowest bending strength. The selected sample "Mix design 1\_milled 8h\_lessSS2x\_no NaOH" has not the highest compressive strength, but it was above 40 MPa while a bending strength of about 15 MPa was achieved.

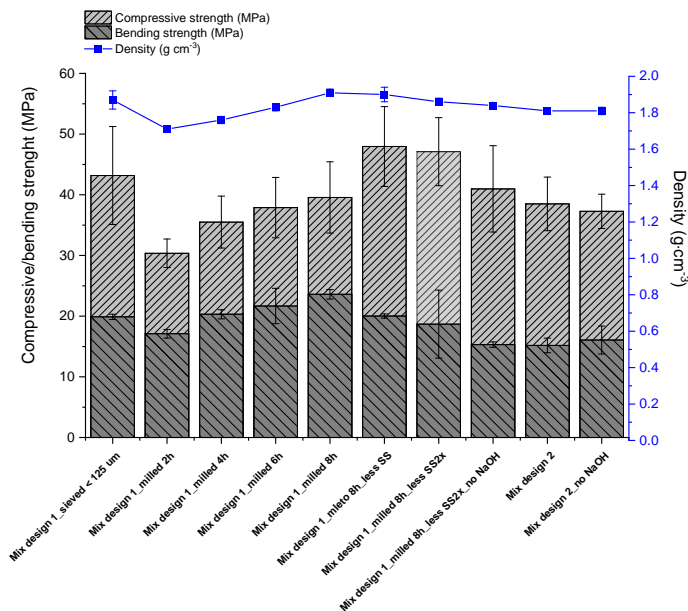


Figure 5: Different experiments were performed to find the optimal mix design. All samples were cured three days in closed bags and then three days at 60 °C and 60% of humidity.

Source: own.

### 3.3 Mix design 3: Variations in mechanical properties and correlations with particle size

Although the optimised mix design (mix design 3; Table 5) resulted in a mix with good workability, there were significant differences in mechanical properties between the different batches, as shown in Figure 6. The average compressive and bending strengths of 30 different prepared panels (made from several different batches) were  $38.5 \text{ MPa} \pm 8.5 \text{ MPa}$  and  $14.9 \text{ MPa} \pm 3.2 \text{ MPa}$ , respectively. Significant differences were also found in the density of the different specimens ( $1.64\text{-}1.91 \text{ g}\cdot\text{cm}^{-3}$ ). Façade panels are required to have a compressive strength of at least 30 MPa (green line in Figure 6) and a bending strength of 10 MPa (grey line in Figure 6). It follows that most of the prepared panels met these requirements (Figure 6). The mechanical property results for 10 randomly selected batches are shown in Figure 7, along with particle size distribution analyses. However, the large differences between the different sample batches are due to the not consistent grinding of the mineral wool used to produce the panels (Figure 7). Although additional grinding in

Termit was performed, the large differences in particle size distribution between the batches affect the workability of the mixture and thus change the mechanical properties between the batches. A significant increase in compressive strength was observed when the smallest fraction ( $< 63 \mu\text{m}$ ) was present in amounts of around 50 wt% (or more). Moreover, the workability of the mixture was better and the compressive strength higher (reaching up to 64 MPa) when the proportion of the smallest fraction in the mixture was higher ( $< 63 \mu\text{m}$ ), as can be seen in **Figure 7**. The bending strength, on the other hand, is not necessarily related to the particle size distribution, since larger fibres could actually help improve the bending strength. Even with a smaller amount of the finer fraction (and thus an increased number of particles larger than  $250 \mu\text{m}$ ), the mechanical properties met the desired values previously determined.

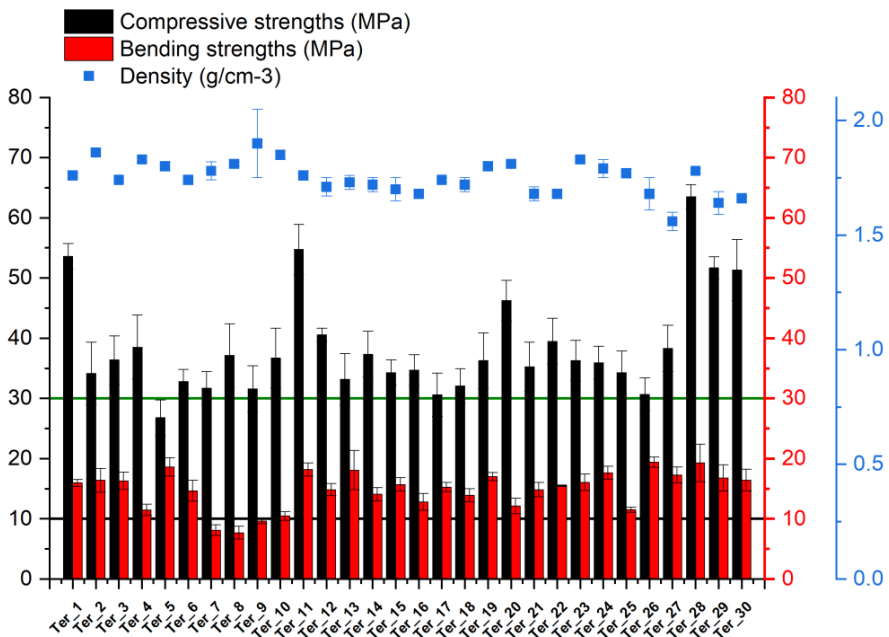


Figure 6: Compressive strength, bending strength and density of 30 different façade panels produced using the mix design 3. The values required are 30 MPa for compressive strength (green line) and 10 MPa for bending strength (grey line).

Source: own.

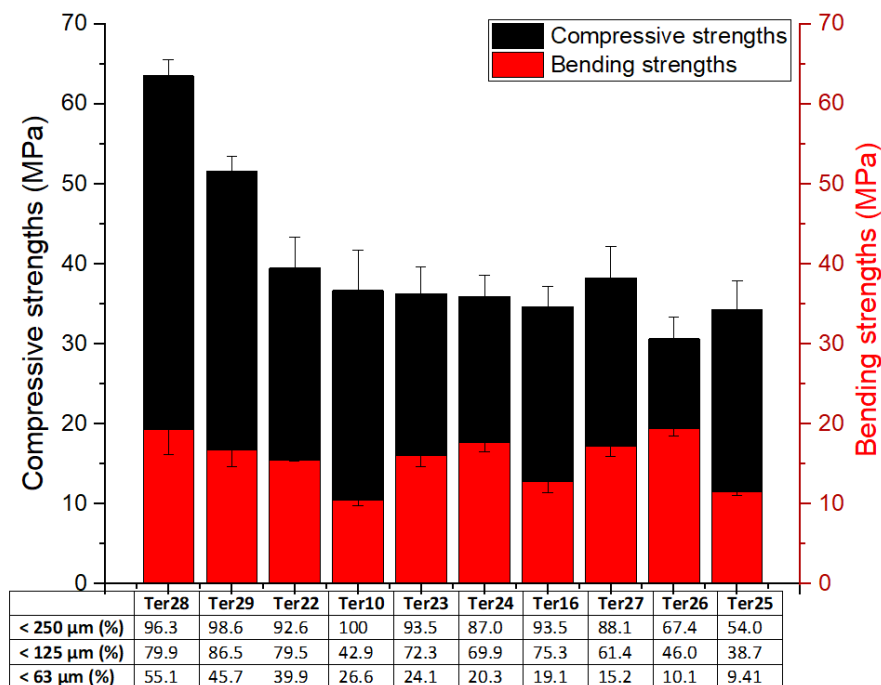


Figure 7: The graph shows the compressive and bending strengths of 10 randomly selected mixtures where the particle size distribution was measured. The particle size distribution for particles sized < 63, < 125 and < 250 µm are provided in the table below the graph. The samples are arranged in descending order of proportion under 63 µm.

Source: own.

### 3.4 The results of selected mixtures: FTIR, open porosity, XRD and leaching of toxic trace and minor elements

In the next step, 12 different batches were selected from mixtures that exhibited different mechanical properties (30 different batches presented in Figure 6), and FTIR, open porosities, XRD and leaching analyses were performed.

The results of the FTIR analysis are provided in Figure 8. A transmission band at around 1644  $\text{cm}^{-1}$  indicates the presence of an H–O–H bending vibration, due to the presence of water in the AAM. The humidity of these samples ranged between 4.0-5.6 wt% (measured after 28 days). In all samples, bands were seen at approximately 1450  $\text{cm}^{-1}$  corresponding to the asymmetric stretching of  $\text{CO}_3^{2-}$  (O–

C–O), and a weak shoulder at around  $\sim 880 \text{ cm}^{-1}$  due to the out-of-plane bending of  $\text{CO}_3^{2-}$ . This could be due to the presence of carbonate in the local slag precursor used in the mixture, and/or as a consequence of the carbonation process presented during the production of the façade panels (Yu et al., 1999). The main Si-O-T band (T = Si, Al) is between 990 and 1000  $\text{cm}^{-1}$ . The shifts of the main Si-O-T bands, compressive strengths and open porosity of the samples are shown in Table 4. There is no correlation between the compressive strength and the band shift as well as with porosity values, suggesting that the alkali activation process (degree of polymerization) is similar for all samples and that the differences in mechanical properties are due to the different particle sizes distributions of the ground material.

**Table 4: Compressive strengths, the position of the Si-O-T (T = Si, Al) asymmetric stretching vibration band and the data for open porosity.**

Sample	Ter 11	Ter 12	Ter 13	Ter 14	Ter 15	Ter 16	Ter 17	Ter 18	Ter 19	Ter 20	Ter 21	Ter 22
Compressive strength	54.8	40.6	33.2	37.3	34.3	34.7	30.6	32.1	36.3	46.3	35.3	39.5
Si-O-T (T = Si, Al) (nm)	1000	999	991	1000	994	999	996	999	998	995	995	990
Open porosity (%)	18.8	24.4	22.1	24.9	21.5	17.9	24.0	15.6	21.4	20.5	26.5	27.8

C-A-S-H and/or C-S-H gels may form due to the presence of lime and local slag, whereas N-A-S-H is typically formed in the alkali-activated metakaolin. In stone wool activated with sodium silicate, however, (N,C)-A-S-H gel is suggested to be the prevailing form (Yliniemi et al., 2020). Since the mixture is composed of several precursors, the position of the bands, which were seen across all the samples, regardless of the batch, could belong to a mixture of gels (C-A-S-H, N-A-S-H (Garcia-Lodeiro et al., 2011) and (N,C)-A-S-H). Since quartz was used as an additional aggregate in the mixture, a doublet is seen at 797 and 778  $\text{cm}^{-1}$ , as well as an additional band at 694  $\text{cm}^{-1}$ .

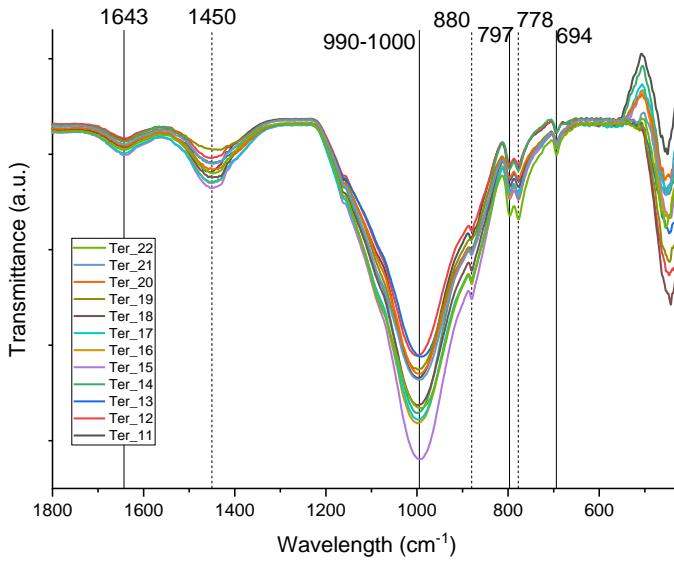


Figure 8: FTIR spectra of 12 different alkali activated façade panels cured at room temperature for three days, followed by three days of curing at 60° C. Source: own.

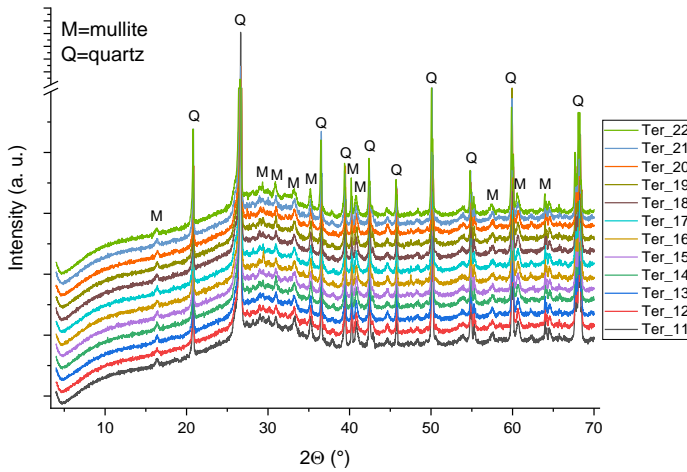


Figure 9: X-ray diffraction patterns of 12 different alkali activated façade panels cured at room temperature for three days followed by three days at 60 °C. Source: own.

12 different X-ray diffraction patterns of alkali-activated façade panels are shown in Figure 9. The amount of amorphous content is around 80 wt% in all the samples (an amorphous halo is observed at the same position in all samples between 22° in 38°). Crystal phase, representing about 20 wt% of all panel material, is primarily consisted of mullite and quartz.

The leaching results of toxic elements from 12 randomly selected façade panels are presented in Table 5. Most of the elements are below the upper limits for inert waste (concentrations of elements measured in the samples are shown in Table 5, and the requirements are provided in Table 6). Cr, As and Sb exceeded this limit in some cases, however, while Mo was above the limit in all cases. Cu did not exceed the limit values set by the Decree on Waste Landfill, but Slovenian regulations are slightly stricter when waste material is intended for recycling, meaning the leached concentrations of Cu are above the values permitted within Slovenia.

**Table 5: Concentrations of toxic metals from 12 different façade panels. Concentrations coloured in red are above the limits stated in the Decree on Waste Landfill, whereas the values in blue show the concentrations of elements that exceeded the required values outlined in the Decree on Waste.**

Element (mg/kg)	Cr	Co	Ni	Cu	Zn	As	Se	Mo	Cd	Sb	Ba	Hg	Pb
Ter_11	0.54	0.01	0.23	0.64	0.09	0.59	0.06	1.16	0.002	0.05	0.13	0.005	0.11
Ter_12	0.56	0.02	0.34	0.98	0.05	0.47	0.06	1.09	0.001	0.03	0.11	0.004	0.04
Ter_13	0.48	0.02	0.30	1.19	0.04	0.45	0.06	0.95	0.001	0.04	0.07	0.004	0.05
Ter_14	0.50	0.01	0.23	0.47	0.02	0.55	0.06	1.04	0.001	0.04	0.08	0.003	0.03
Ter_15	0.40	0.02	0.256	1.00	0.01	0.39	0.04	0.72	0.001	0.04	0.07	0.004	0.04
Ter_16	0.51	0.01	0.31	0.87	0.03	0.27	0.04	0.89	<0.001	0.02	0.05	0.004	0.05
Ter_17	0.46	0.01	0.26	0.82	0.02	0.30	0.04	0.91	<0.001	0.02	0.05	0.003	0.03
Ter_18	0.39	0.02	0.17	0.41	0.05	0.32	0.04	0.90	<0.001	0.03	0.08	0.003	0.04
Ter_19	0.37	0.02	0.19	0.92	0.03	0.34	0.04	0.92	0.001	0.04	0.05	0.003	0.06
Ter_20	0.38	0.02	0.22	0.77	0.01	0.47	0.04	0.82	<0.001	0.04	0.06	0.003	0.02
Ter_21	0.42	0.01	0.22	0.83	0.02	0.37	0.04	0.75	<0.001	0.04	0.06	0.003	0.04
Ter_22	0.51	0.01	0.22	0.58	0.05	0.64	0.04	0.93	<0.001	0.12	0.20	0.004	0.08

A comparison was also made between the leaching of elements from the façade panel prepared from mix design 1 and that prepared using the current formula (mix design 3), which shows a decrease in the concentrations of most of the toxic elements (Table 7). Significant decreases are observed in the case of Cu and Mo. The addition of a smaller amount of sodium silicate, and the absence of NaOH, could lead to a slight reduction in the pH of the solution, which could influence the leaching potential of these two elements. However, curing conditions at 60 °C



instead of room temperature may also improve the immobilisation of those two elements (Izquierdo et al., 2010; Keulen et al., 2018).

**Table 6: The concentrations of inert and non-hazardous waste that should not be exceeded according to the Decree on Waste Landfill, and the limit on elemental concentrations that can be used in recycled products based on data from the Slovene Decree on Waste.**

Element (mg/kg)	Cr	Co	Ni	Cu	Zn	As	Se	Mo	Cd	Sb	Ba	Hg	Pb
Inert waste	10.0	/	10.0	50.0	50.0	2.0	0.5	10.0	3	0.7	100.0	0.20	10.0
Non-hazardous waste	0.5	0.03	0.4	0.5	2.0	0.1	0.6	0.5	0.025	0.3	5.0	0.005	0.5
Decree on waste (SLO)	0.5	/	0.4	2.0	4.0	0.5	0.1	0.5	0.04	0.06	20.0	0.01	0.5

**Table 7: A comparison of the toxic metals leached from the final mix design (mix design 3) and the first mix developed in the lab. The concentrations coloured in red are above the required values stated in the Decree on Waste Landfill, whereas the values in blue are the elemental concentrations that exceeded the values required according to the Decree on Waste.**

Element (mg/kg)	Cr	Co	Ni	Cu	Zn	As	Se	Mo	Cd	Sb	Ba	Hg	Pb
Mix design 1	0.65	0.04	0.83	2.60	0.15	0.54	0.16	1.69	0.003	0.04	0.25	0.005	0.09
Mix design 3	0.46 ± 0.10	0.015 ± 0.005	0.25 ± 0.05	0.79 ± 0.23	0.04 ± 0.02	0.43 ± 0.12	0.05 ± 0.01	0.92 ± 0.13	0.0008 ± 0.0004	0.04 ± 0.02	0.08 ± 0.04	0.004 ± 0.001	0.05 ± 0.02

### 3 Conclusions

The façade panels prepared varied in terms of their mechanical properties as a result of the unevenly milled batches of (pre-milled) mineral wool. If a higher proportion of smaller fractions are present in the mixture, the mechanical properties are better. There is, however, no correlation between the mechanical properties of the panels and the degree of polymerization, open porosities and the leaching parameters – an improvement in mechanical properties does not necessarily lead to an improvement in the immobilization of elements, as other processes, such as diffusion and dissolution, may affect the leaching of elements. With a slight modification to the mix design and a change in the curing conditions, the leached concentrations of most

toxic elements were reduced. This is significantly important for Cr, Ni, Cu, As, Se, Mo and Hg, all of which exceeded the permitted values outlined in the Decree on Waste Landfill and the Decree on Waste. Additional modifications to the mix design and curing process should, however, be tested, in order to reduce the concentrations of those elements to below the limit values required for recycled products. Further work with respect to the composition of samples is, however, needed, to ensure the mixture is suitable for use as a commercially-available recycled product.

### Acknowledgments

This project has received funding from the European Union's EU Framework Programme for Research and Innovation, Horizon 2020, under Grant Agreement #821000. We acknowledge financial support from the Slovenian Research Agency, Slovenia, through project No. Z2-3199 »The immobilisation and leaching of toxic trace elements in alkali-activated materials prepared from locally available waste and by-products«.

### References

- Garcia-Lodeiro, I., Palomo, A., Fernández-Jiménez, A., Macphee, D.E., 2011. Compatibility studies between N-A-S-H and C-A-S-H gels. Study in the ternary diagram Na<sub>2</sub>O–CaO–Al<sub>2</sub>O<sub>3</sub>–SiO<sub>2</sub>–H<sub>2</sub>O, *Cem. Concr. Res.* 41, 923-931.  
<https://doi.org/https://doi.org/10.1016/j.cemconres.2011.05.006>.
- Izquierdo, M., Querol, X., Phillipart, C., Antenucci, D., Towler, M., 2010. The role of open and closed curing conditions on the leaching properties of fly ash-slag-based geopolymers, *J. Hazard. Mater.* 176, 623-628.
- Keulen, A., van Zomeren, A., Dijkstra, J.J., 2018. Leaching of monolithic and granular alkali activated slag-fly ash materials, as a function of the mixture design, *Waste Manag.* 78, 497-508.  
<https://doi.org/https://doi.org/10.1016/j.wasman.2018.06.019>.
- Kinnunen, P., Yliniemi, J., Talling, B., Illikainen, M., 2017. Rockwool waste in fly ash geopolymer composites, *J. Mater. Cycles Waste Manag.* 19, 1220-1227.  
<https://doi.org/10.1007/s10163-016-0514-z>.
- Kowatsch, S., 2010, *Mineral Wool Insulation Binders BT - Phenolic Resins: A Century of Progress*, en: L. Pilato (Ed.), Springer Berlin Heidelberg, Berlin, Heidelberg: p. 209-242.  
[https://doi.org/10.1007/978-3-642-04714-5\\_10](https://doi.org/10.1007/978-3-642-04714-5_10).
- Müller, A., Leydolph, B., Stanelle, K., 2009. Recycling Mineral Wool Waste: Technologies for the Conversion of the Fiber Structure, Part 1, *Interceram.* 58, 378-381.
- Official Gazette of Republic Slovenia, 2014. Decree on Waste Landfill, Nos. 2020, 10/14, 54/15, 36/16, 37/18. <https://www.ecolex.org/details/legislation/decreed-on-the-landfill-of-waste-lex-faoc130542/>.
- Pavlin, M., Horvat, B., Frankovič, A., Ducman, V., 2021a. Mechanical, microstructural and mineralogical evaluation of alkali-activated waste glass and stone wool, *Ceram. Int.*  
<https://doi.org/https://doi.org/10.1016/j.ceramint.2021.02.068>.
- Pavlin, M., Horvat, B., Ducman, V., 2021b. Challenges at upscaling from laboratory to industrial level in Wool2Loop project, en: *Technol. Bus. Model. Circ. Econ.*, Portorož (Slovenia), p. 35.  
[http://tbmce.um.si/wp-content/uploads/2021/09/02\\_TBMCE2021\\_Book\\_of\\_Abstacts.pdf](http://tbmce.um.si/wp-content/uploads/2021/09/02_TBMCE2021_Book_of_Abstacts.pdf).

- Pavlin, M., Horvat, B., Ducman, V., 2022. Preparation of façade panels based on alkali-activated waste mineral wool, their characterization and durability aspects, *Int. J. Appl. Ceram. Technol.* n/a. <https://doi.org/https://doi.org/10.1111/ijac.13998>.
- Väntsi, O., Kärki T., 2014. Mineral wool waste in Europe: A review of mineral wool waste quantity, quality, and current recycling methods, *J. Mater. Cycles Waste Manag.* 16, 62-72. <https://doi.org/10.1007/s10163-013-0170-5>.
- Yliniemi, J., Kinnunen, P., Karinkanta, P., Illikainen, M., 2016. Utilization of Mineral Wools as Alkali-Activated Material Precursor, *Materials (Basel)*. 9, 312. <https://doi.org/10.3390/ma9050312>.
- Yliniemi, J., Walkley, B., Provis, J.L., Kinnunen, P., Illikainen, M., 2020. Nanostructural evolution of alkaliactivated mineral wools, *Cem. Concr. Compos.* 106, 103472. <https://doi.org/10.1016/J.CEMCONCOMP.2019.103472>.
- Yu, P., Kirkpatrick, R.J., Poe, B., McMillan, P.F., Cong, X., 1999. Structure of Calcium Silicate Hydrate (C-S-H): Near-, Mid-, and Far-Infrared Spectroscopy, *J. Am. Ceram. Soc.* 82, 742-748. <https://doi.org/10.1111/j.1151-2916.1999.tb01826.x>.

